Applications of 2D full waveform inversion at different spatial scales

presented at the structural modelling and geophysics workshop, Nancy

Thomas Bohlen, Laura Gassner (PhD), Lingli Gao (Post-Doc), Tobias Gerach (Msc), Peter Habelitz (Msc),Thomas Hertweck (Post-Doc), Valerie Krampe (Msc), Daniel Krieger (Msc), Fabian Kühn (Msc), Tilman Metz (PhD), Yudi Pan (Post-Doc), Renat Shigapov (PhD), Niklas Thiel (PhD)

Geophysical Institute, Department of Physics

25.04.2019

Streamer	OBS/OBC	Near Surface	Medical Imaging
			
Target Depth: 4km	Target Depth: 2km	Target Depth: 10m	Target Depth: 10cm
Max. Offset: 80λ	Max. Offset: 200 λ	Max. Offset: 20λ	Max. Offset: 330 λ

Agenda

Goals of FWI

Early days: Find all possible earth models that explain the full data by full wave modelling !

Today: Find one discrete numerical computer model that predicts the relevant signals at low frequencies

Goals of FWI

Early days: Find all possible earth models that explain the full data by full wave modelling !

Today: Find one discrete numerical computer model that predicts the relevant signals at low frequencies

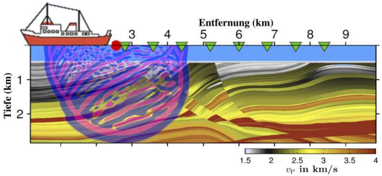

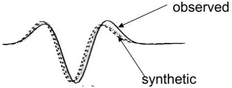

P–waves
S–waves
Surface waves

Goals of FWI

Early days: Find all possible earth models that explain the full data by full wave modelling !

Today: Find one discrete numerical computer model that predicts the relevant signals at low frequencies

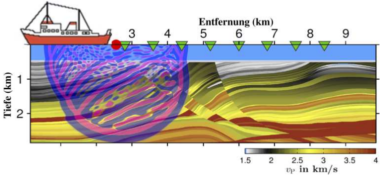

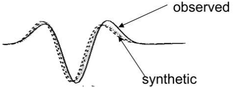

P–waves
S–waves
Surface waves

Benefits

1. **Improved resolution:** $\approx \frac{\lambda}{2}$
2. **Possibility of multi-parameter reconstruction:**
   a. P-wave velocity
   b. S-wave velocity
   c. Attenuation
   d. Anisotropy
   e. Density
3. **Future petrophysical characterization of rocks**

Applications of FWI

In recent 20 years FWI has received great attention and has been applied sucessfully to a broad range of spatial scales and wave types

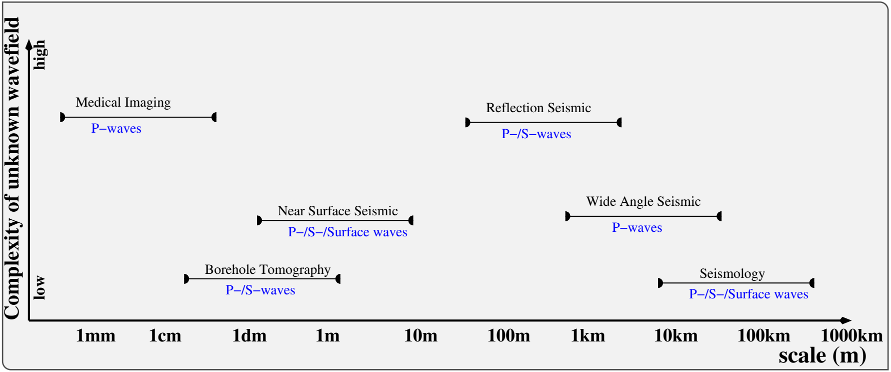

Applications of FWI

In recent 20 years FWI has received great attention and has been applied sucessfully to a broad range of spatial scales and wave types

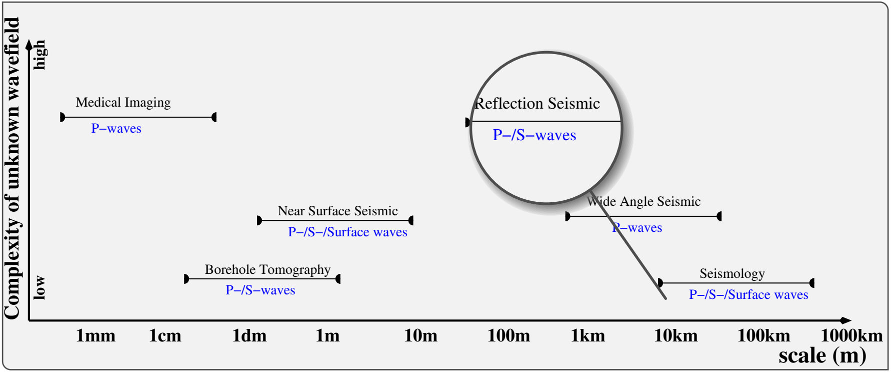

Example 1: Top salt imaging using streamer data
Target depth: 3-4 km, Acoustic-Elastic, 80 λ

Applications of FWI

In recent 20 years FWI has received great attention and has been applied sucessfully to a broad range of spatial scales and wave types

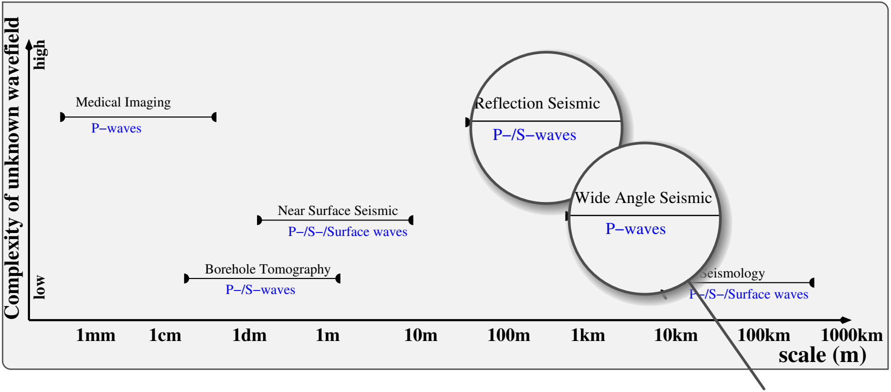

Example 2: Imaging of gas hydrates using OBS data
Target depth: 1.4-2.0 km, Acoustic, 150 λ

Applications of FWI

In recent 20 years FWI has received great attention and has been applied sucessfully to a broad range of spatial scales and wave types

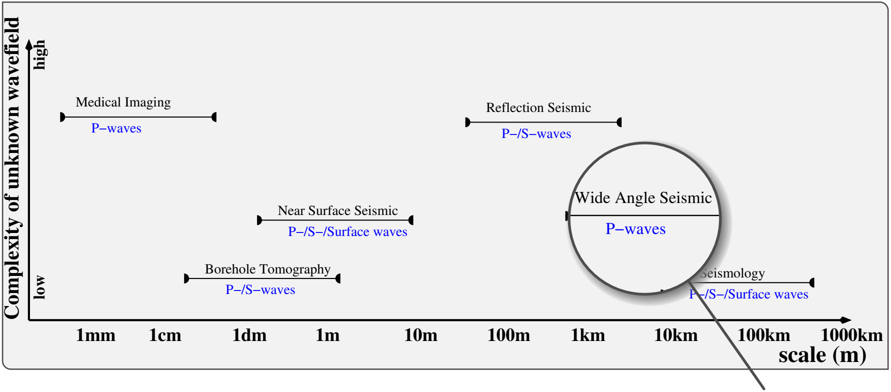

Example 3: Imaging of shallow marine gas hydrates using OBC data
Target depth: 0.15-1.0 km, Acoustic, 200 λ

Applications of FWI

In recent 20 years FWI has received great attention and has been applied sucessfully to a broad range of spatial scales and wave types

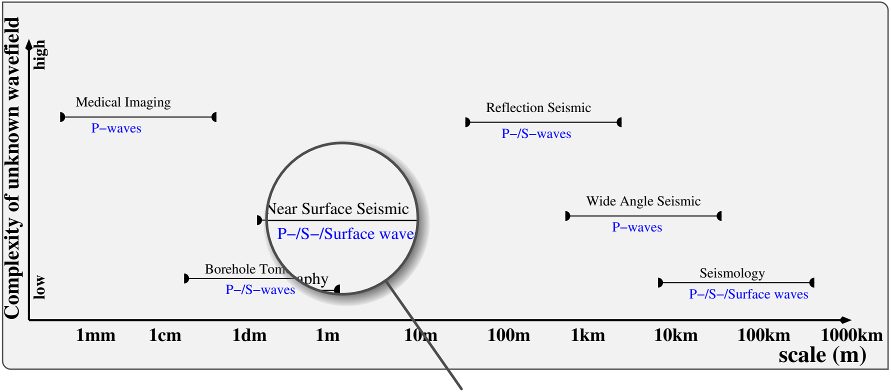

Example 4: Near surface characterizaztion using geophone data (land)
Target depth: 0-20 m, Visco-elastic, 20 λ

Applications of FWI

In recent 20 years FWI has received great attention and has been applied sucessfully to a broad range of spatial scales and wave types

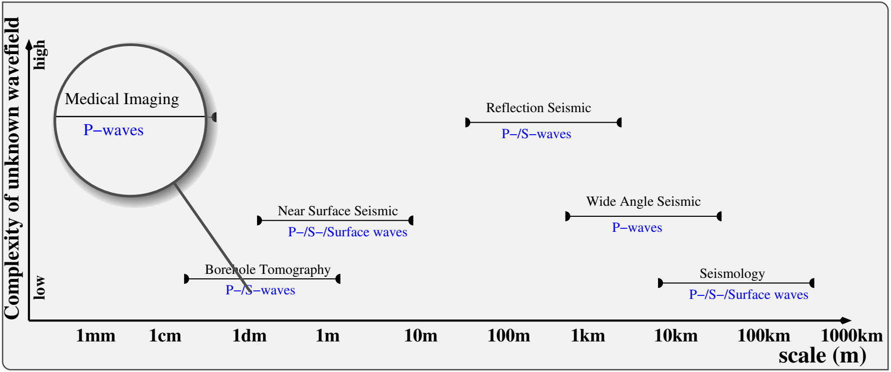

Example 5: Medical imaging (synthetic)
Target depth: 5-15 cm, Visco-acoustic, 330 λ

Agenda

FWI: iterative data fitting procedure

Initial model m_0

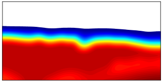

Field data d

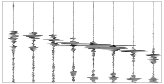

FWI: iterative data fitting procedure

Initial model m_0 → **Forward wavefield**

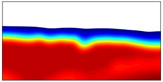

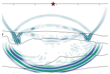

Field data d

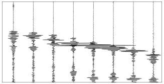

FWI: iterative data fitting procedure

Initial model m_0

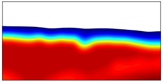

Forward wavefield

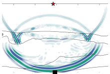

Synthetic data d’

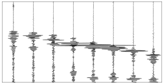

Field data d

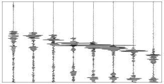

FWI: iterative data fitting procedure

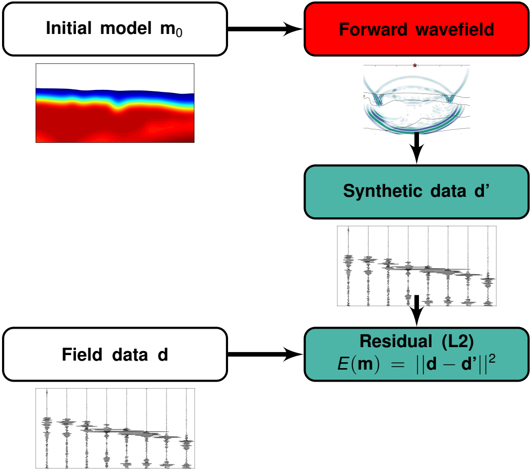

FWI: iterative data fitting procedure

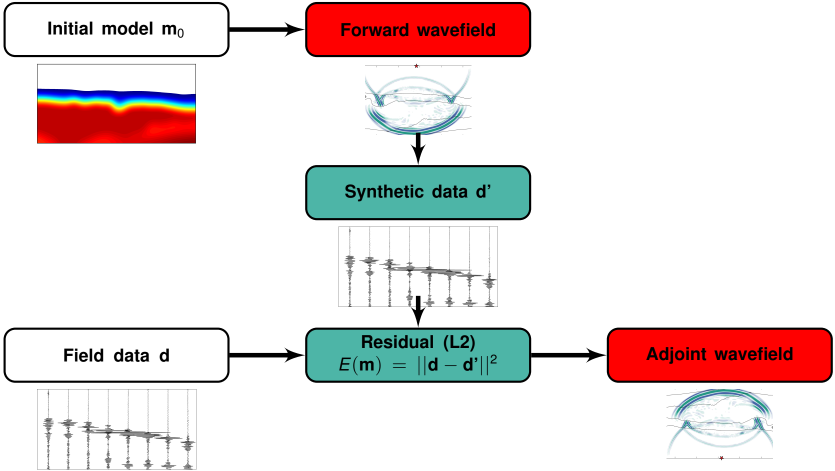

FWI: iterative data fitting procedure

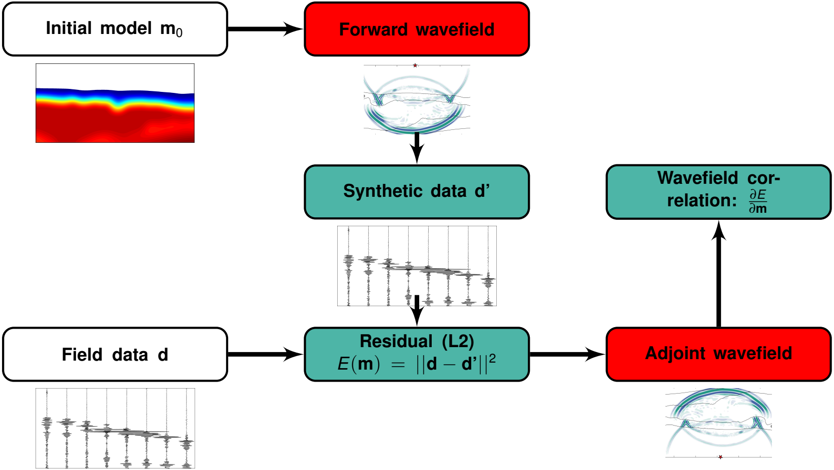

FWI: iterative data fitting procedure

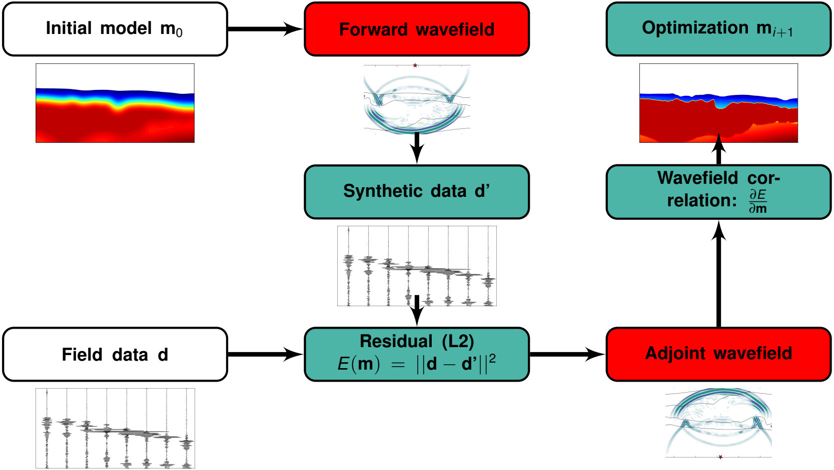

FWI: iterative data fitting procedure

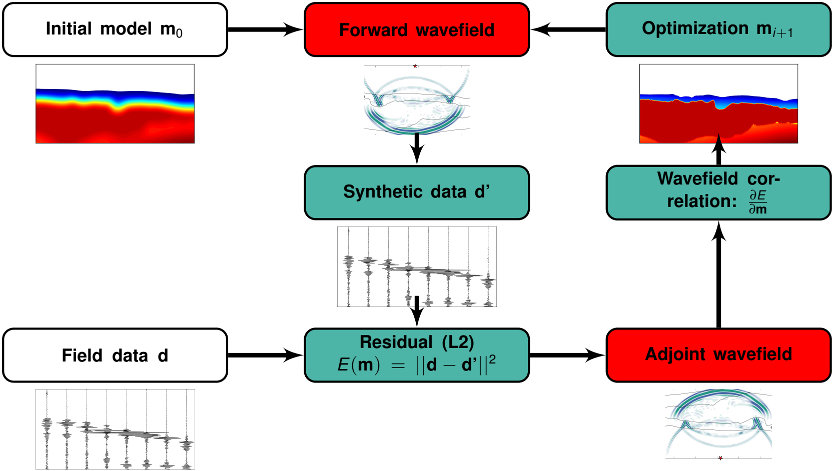

FWI: iterative data fitting procedure

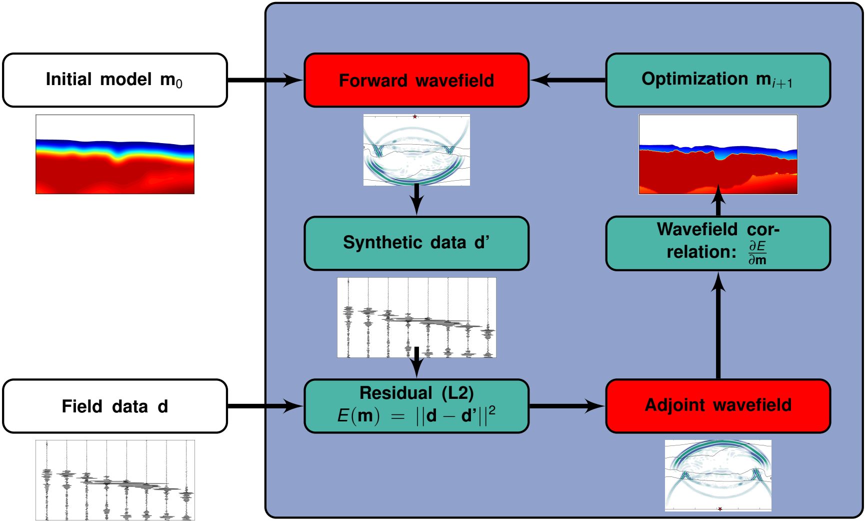

Challenges of FWI (1/7)

Mitigate non-linearities by multi-scale approach

- we need sufficient low wave numbers in the initial model or the observed data

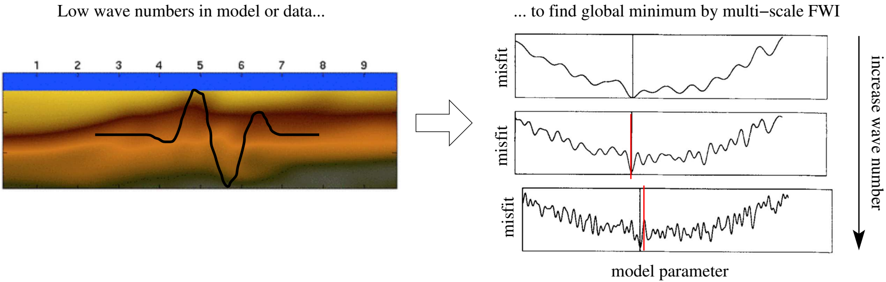

Challenges of FWI (2/7)

Suitable misfit definition

- to measure the misfit of the relevant signals
- **Normalized L2**, envelope, optimal transport,...
- defines the adjoint sources
- tradeoff between robustness (against noise, cycle skipping) and resolution

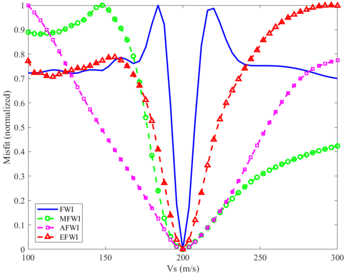

Challenges of FWI (3/7)

Appropriate physics for wave propagation

- to model the relevant signals
- multi-parameter reconstruction
- consider forward and adjoint equations

Acoustic

$$\frac{\partial^2 p}{\partial t^2} = c^2 \left(\frac{\partial^2 p}{\partial x^2} + \frac{\partial^2 p}{\partial y^2} + \frac{\partial^2 p}{\partial z^2} \right)$$

P–waves

Elastic

$$p_{ij} = \lambda \theta \delta_{ij} + 2\mu \epsilon_{ij}$$

$$\epsilon_{ij} = \frac{1}{2} \left(\frac{\partial u_i}{\partial x_j} + \frac{\partial u_j}{\partial x_i} \right)$$

$$\rho \frac{\partial^2 u_i}{\partial t^2} = \frac{\partial p_{ij}}{\partial x_j} + f_i$$

P–waves, S–waves
Surface waves

Visco–elastic

$$\dot{\sigma}_{ij} = \frac{\partial v_k}{\partial x_k} \{ M(1 + L\tau^p) - 2\mu(1 + L\tau^s) \} + 2\frac{\partial v_i}{\partial x_j} \mu (1 + L\tau^s) + \sum_{l=1}^{L} r_{ijl} \quad \text{if } i = j$$

$$\dot{\sigma}_{ij} = \left(\frac{\partial v_i}{\partial x_j} + \frac{\partial v_j}{\partial x_i} \right) \mu (1 + L\tau^s) + \sum_{l=1}^{L} r_{ijl} \quad \text{if } i \neq j \; ,$$

$$\dot{r}_{ijl} = -\frac{1}{\tau_{\sigma l}} \left\{ (M\tau^p - 2\mu\tau^s) \frac{\partial v_k}{\partial x_k} + 2\frac{\partial v_i}{\partial x_j} \mu \tau^s + r_{ijl} \right\} \quad \text{if } i = j \; ,$$

$$\dot{r}_{ijl} = -\frac{1}{\tau_{\sigma l}} \left\{ \mu \tau^s \left(\frac{\partial v_i}{\partial x_j} + \frac{\partial v_j}{\partial x_i} \right) + r_{ijl} \right\} \quad \text{if } i \neq j \; .$$

$$\varrho \frac{\partial v_i}{\partial t} = \frac{\partial \sigma_{ij}}{\partial x_j} + f_i \; ,$$

P–waves, S–waves
Surface waves
Attenuation

→ Computational requirements

Challenges of FWI (4/7)

Numerical solution and space discretization

- **Finite-Differences**, Spectral elements
- Boundary condition (free surface topography is challenge with FD)

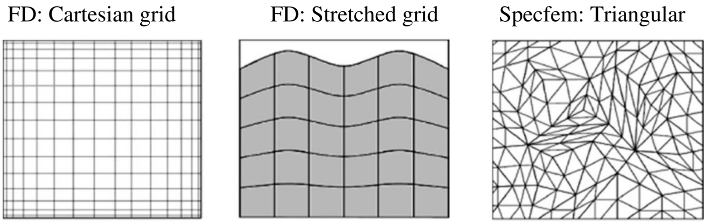

(Igel et al. 2011)

Challenges of FWI (5/7)

Optimization method

- efficient calculation of gradients by the adjoint method
- available methods: steepest-descent, conjugate gradient, L-BFGS, Gauß-Newton, Truncated Newton etc.
- consider global strategy if number of parameters is small (uncertainty estimation)

Gradient–based (local)

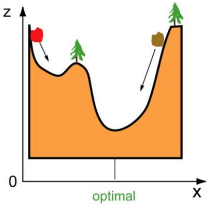

Global

Challenges of FWI (6/7)

High Performance Computing

- Efficient forward and adjoint simulation on heterogeneous architectures (CPU/GPU)

Domain Decomposition

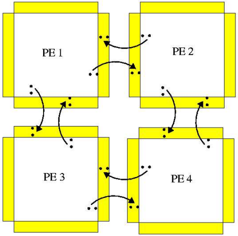

Cluster

(Foto:KIT)

Challenges of FWI (7/7)

Preconditioning - manipulation of the gradient

- smoothing to reduce artifacts at sources/receivers
- enhance regions with poor illumination
- ...

Gradient with preconditioning

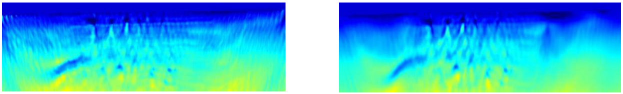

(Habelitz 2017)

Questions ?

Agenda

Acoustic/elastic FWI of marine streamer data

Goal

- Imaging of structures above (and below) a salt dome located west of Africa.

Acquisition geometry

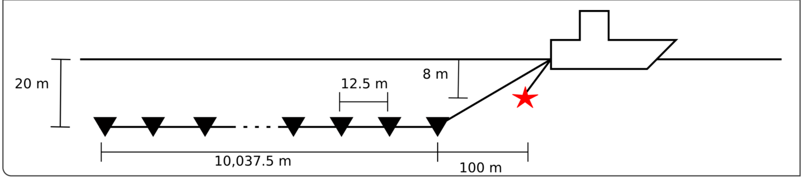

Streamer (length 10 km) record P-waves in the water

(Thiel et al. 2019, Thiel 2018)
Data was provided by PGS

Initial model and field data

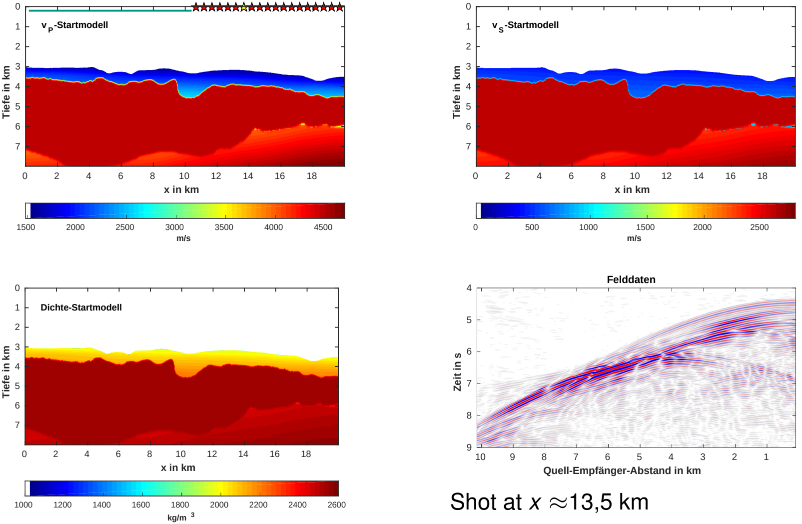

Shot at $x \approx 13{,}5$ km

(Thiel et al. 2019, Thiel 2018)

Acoustic Finite-Difference Simulation

Click to play

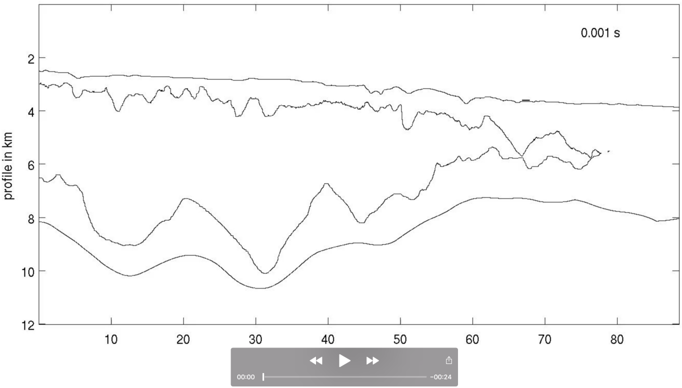

(Thiel et al. 2019, Thiel 2018)

Evolution of pressure in acoustic and elastic simulation

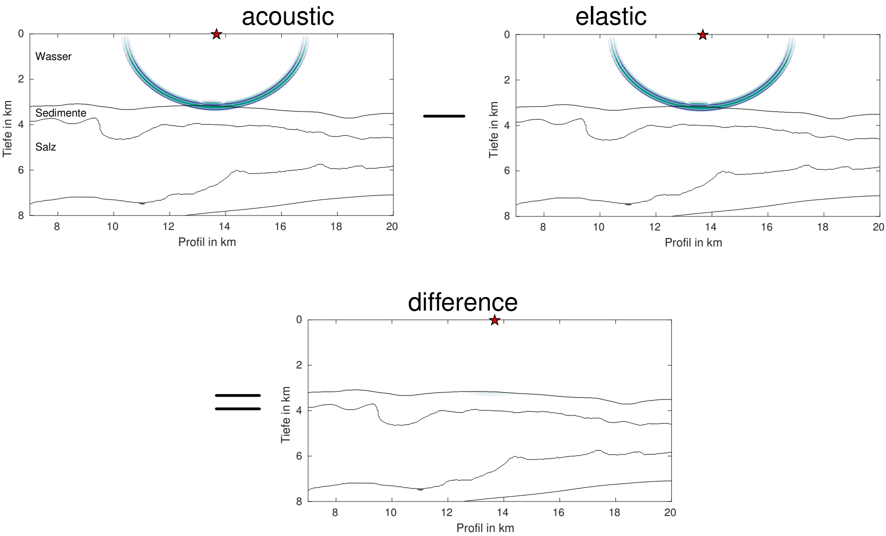

(Thiel et al. 2019, Thiel 2018)

Evolution of pressure in acoustic and elastic simulation

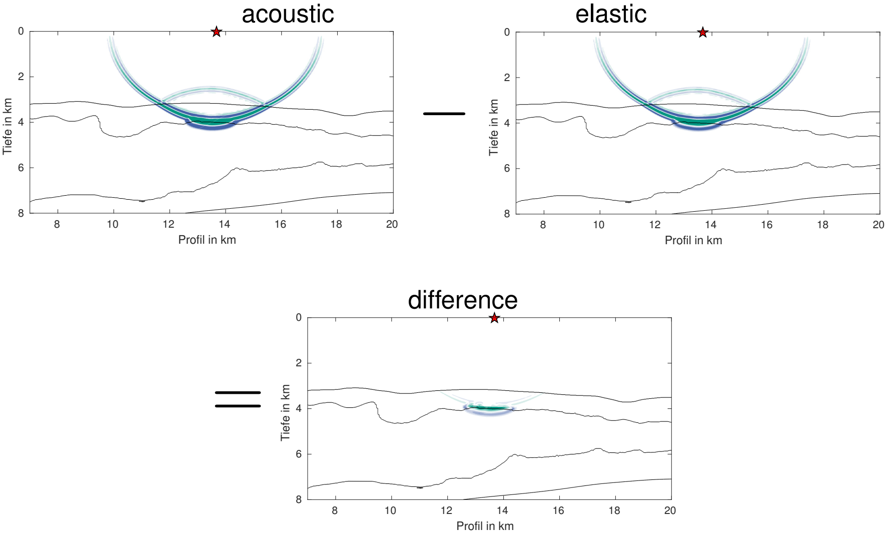

(Thiel et al. 2019, Thiel 2018)

Evolution of pressure in acoustic and elastic simulation

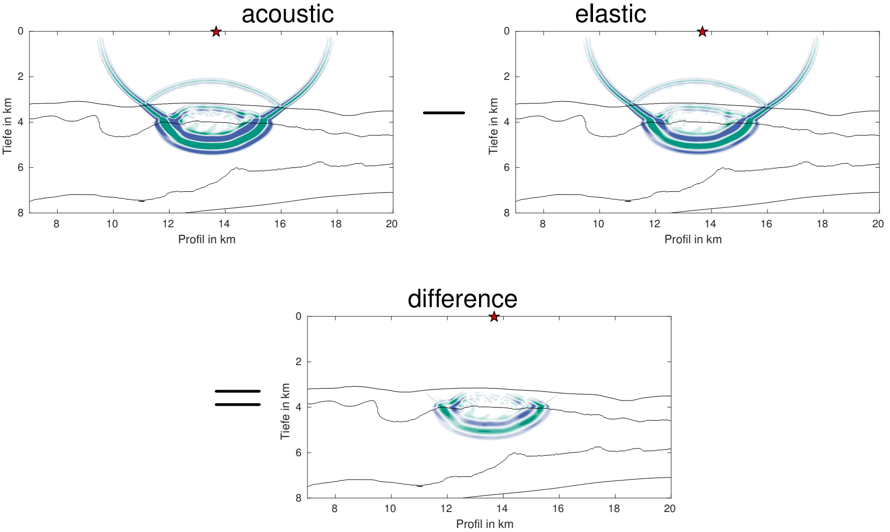

(Thiel et al. 2019, Thiel 2018)

Evolution of pressure in acoustic and elastic simulation

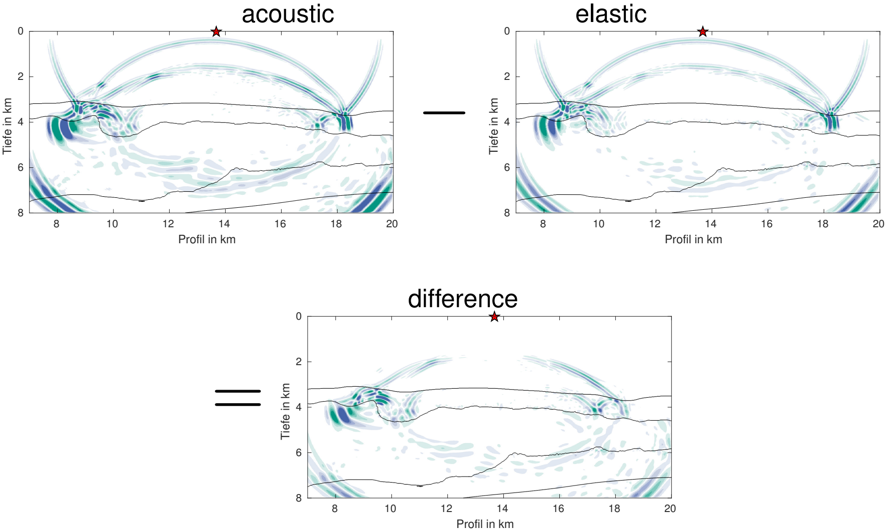

(Thiel et al. 2019, Thiel 2018)

Application of acoustic FWI to field data

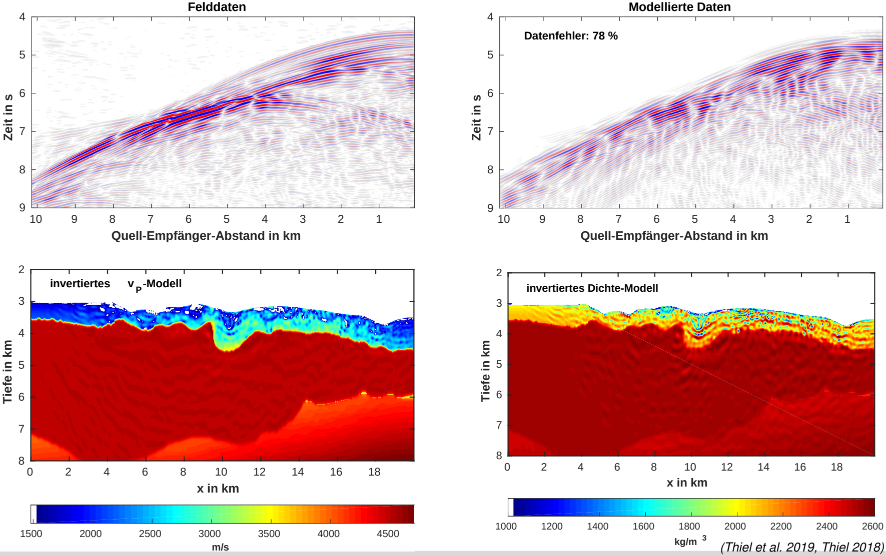

(Thiel et al. 2019, Thiel 2018)

Application of elastic FWI to field data

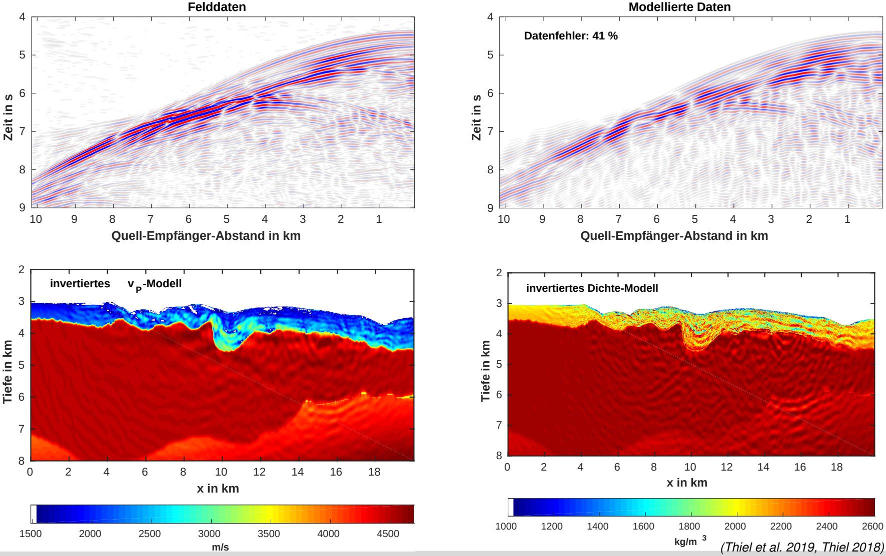

(Thiel et al. 2019, Thiel 2018)

Comparison of acoustic and elastic FWI models

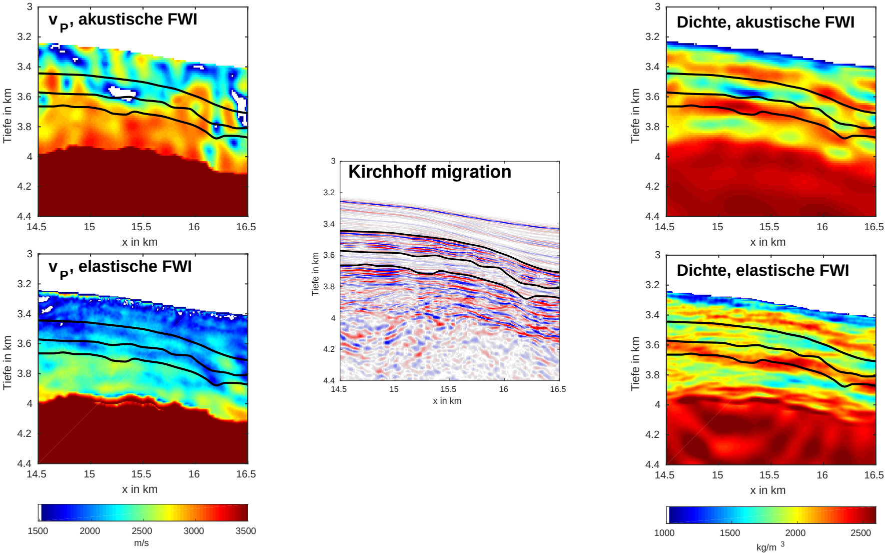

(Thiel et al. 2019, Thiel 2018)

Acoustic/elastic FWI of marine streamer data for top-salt imaging

Conclusions

- Elastic FWI may be necessary even in marine environment in the presence of strong contrast discontinuities such as salt
- The discontinuities in the P-velocity (and density) show similarities to the reflectivity seen in migrated images

Questions ?

Agenda

Karlsruhe Institute of Technology

Seismic characterization of marine gas hydrates

Gas hydrate properties

- Store huge amounts of natural gas
- Mainly found at continental margins and permafrost
- Gas can be trapped beneath hydrated sediments if stability conditions are met
- Increase/decrease of V_p in hydrates/gas
- Hydrate-gas contact creates BSR

Gas hydrates

Source: https://de.wikipedia.org/wiki/Gashydrat

Goal of FWI: Improvement of P-wave velocity model

Acoustic FWI of OBS data from the Black Sea

OBS profiles

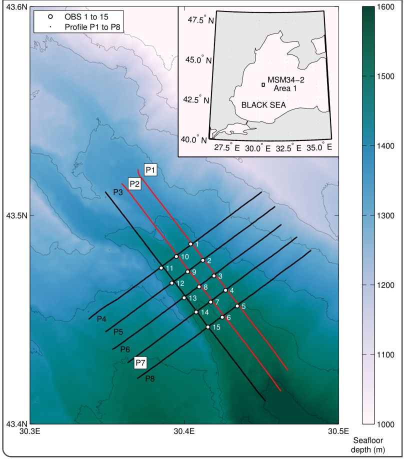

Streamer data P1

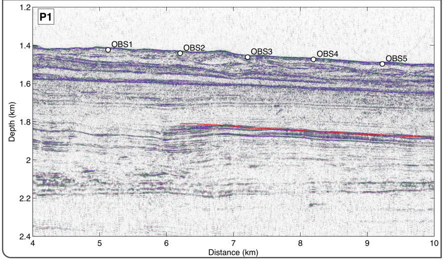

BSR at 400m bsf

(Gassner et al. 2019, Gassner 2018)

Acoustic FWI of OBS data from the Black Sea

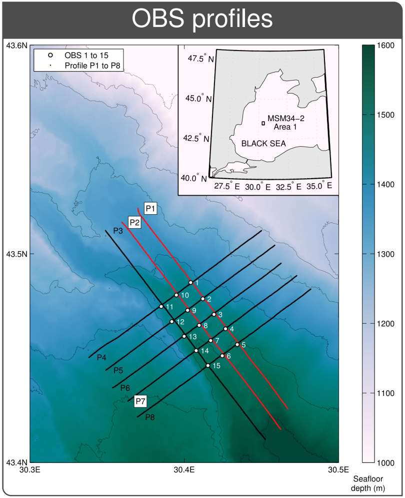

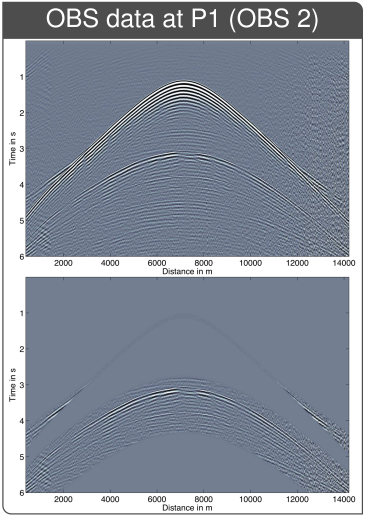

full and reduced data

(Gassner et al. 2019, Gassner 2018)

Acoustic FWI of OBS data from P1

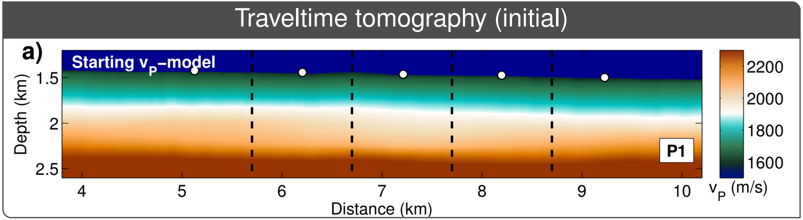

(Gassner et al. 2019, Gassner 2018)

Acoustic FWI of OBS data from P1

Karlsruhe Institute of Technology

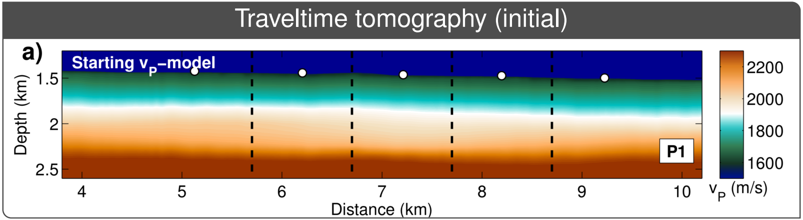

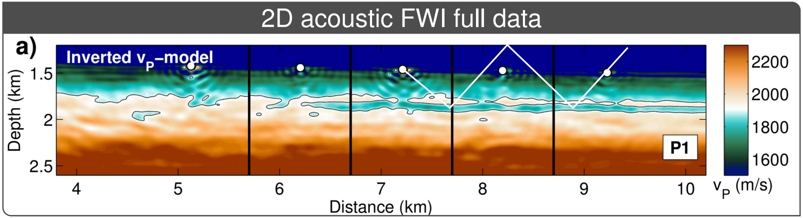

→ improved resolution of FWI compared to traveltime tomography

(Gassner et al. 2019, Gassner 2018)

Acoustic FWI of OBS data from P1

2D acoustic FWI full data

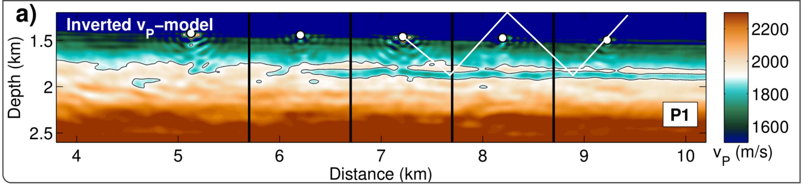

2D acoustic FWI reduced data

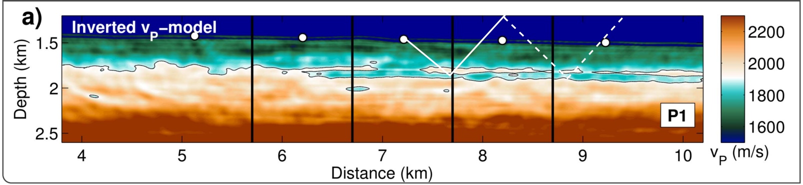

→ Artefacts are removed when using reduced data

(Gassner et al. 2019, Gassner 2018)

Data fit

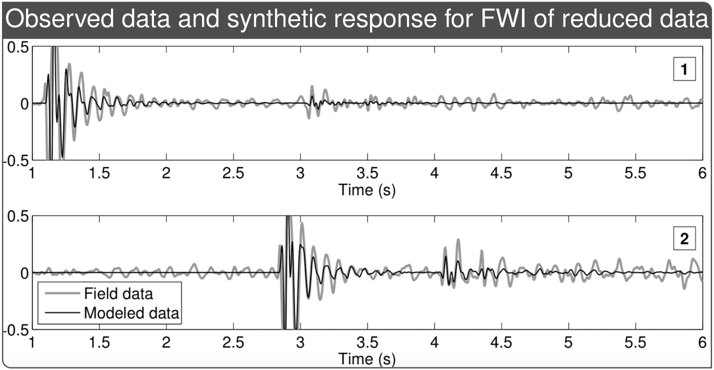

moderate fit of primary and multiple reflections

(Gassner et al. 2019, Gassner 2018)

Seismic characterization of marine gas hydrates by FWI

Conclusions

- Models of acoustic FWI show improved resolution compared to traveltime tomography
- FWI of multiples and refracted waves (only) show less artefacts around OBS

Questions ?

Agenda

FWI of OBC data in shallow water

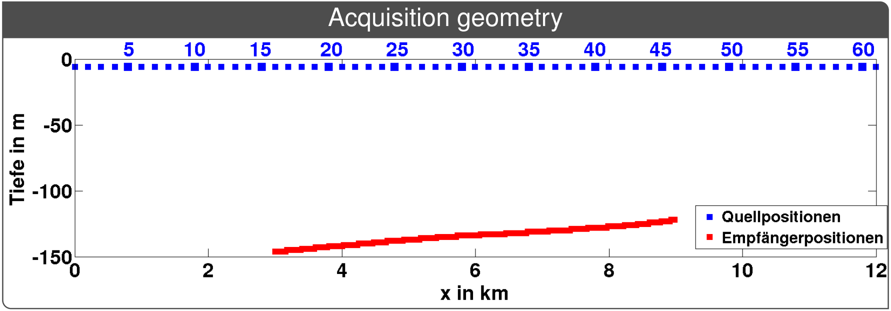

- Ocean-Bottom-Cable
- Length: 6 km, 240 Hydrophones
- 61 Airgun shots
- Water depth approx. 130m
- Maximum offset 9 km

(Kunert 2015, Kunert et al. 2016, Habelitz 2017)
Data was provided by Addax

FWI of OBC data in shallow water

Acoustic simulation of wavefield in the final FWI model

Click to play

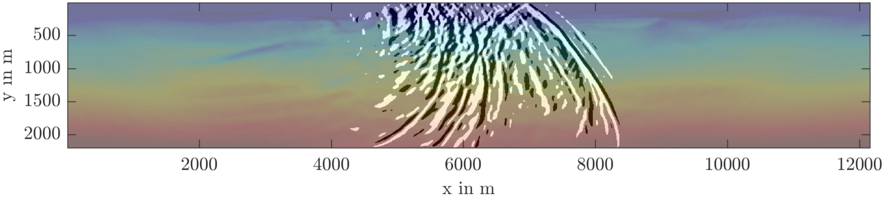

(Habelitz 2017)

FWI of OBC data in shallow water

Shot gather

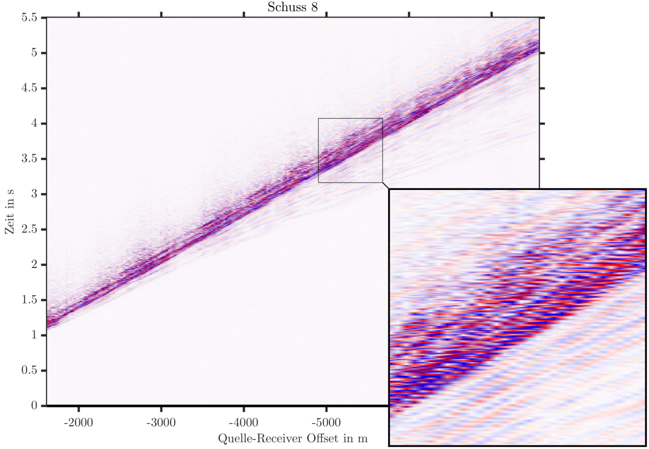

(Habelitz 2017)

FWI of OBC data in shallow water

Acoustic modes

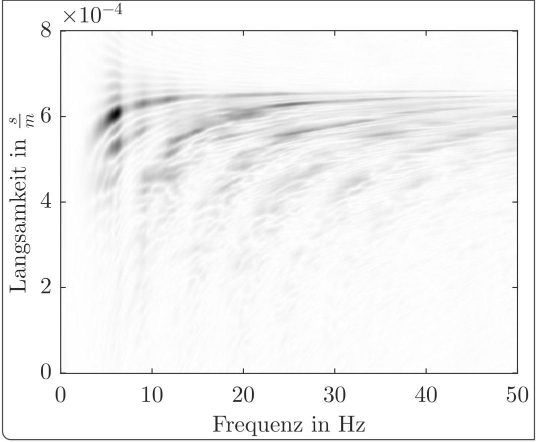

(Habelitz 2017)

FWI of OBC data in shallow water

Performance of FWI

Click to play

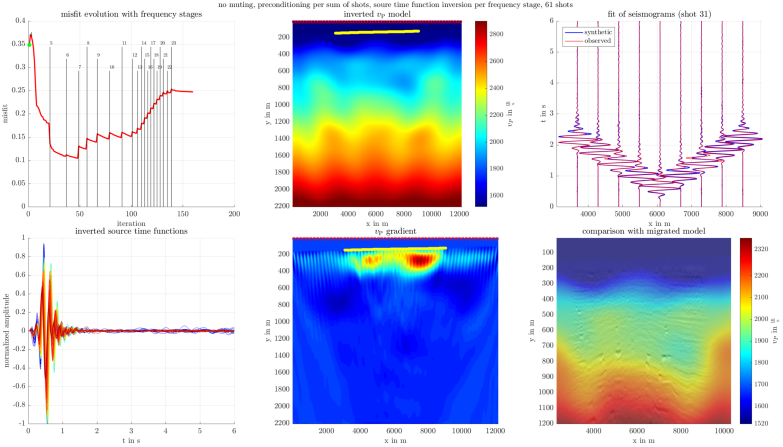

(Habelitz 2017)

FWI of OBC data in shallow water

Data fit

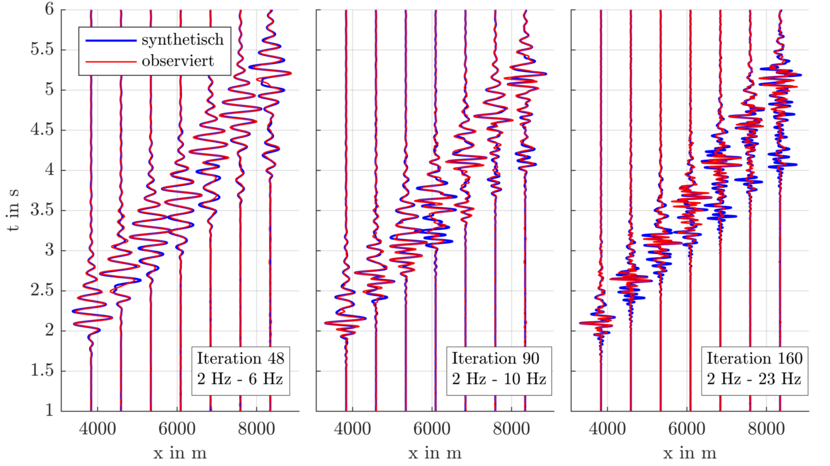

(Habelitz 2017)

FWI of OBC data in shallow water

Final model

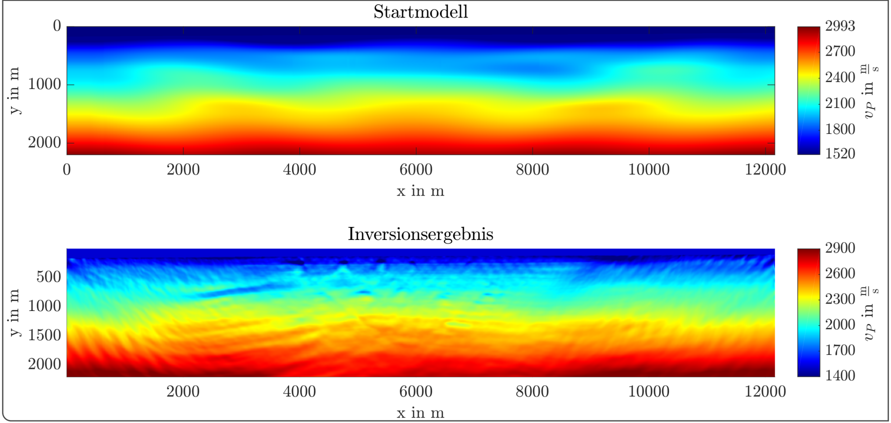

(Habelitz 2017)

FWI of OBC data in shallow water

Final model

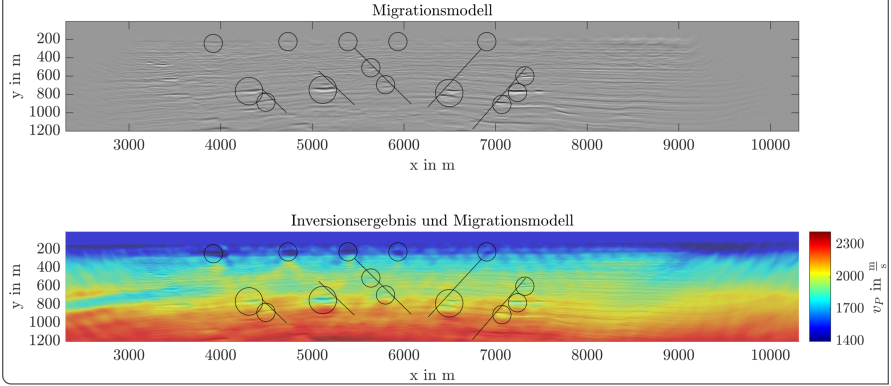

(Habelitz 2017)

FWI of OBC data in shallow water

Conclusions

- Acoustic FWI of guided waves in shallow water was successful
- Higher resolution of Vp model reveals gas accumulations and pathways along faults
- Consistent with migrated images of reflected waves (independent data)

Questions ?

Agenda

1. Introduction

2. Methodology and Challenges

3. Applications of FWI

3.1 Top-salt imaging using streamer data

3.2 Marine gas hydrates using OBS data

3.3 Shallow marine gas using OBC data

3.4 Near surface characterization using surface waves

3.5 Medical imaging

4. Conclusions

Visco-elastic FWI for near surface characterization

Shallow seismic surface and body waves are useful for geotechnical site characterization

- easily excited by a hammer blow
- surface waves are strong signals
- highly sensitive for S-wave velocity
- depth of investigation up to 30-40 m

Field data acquisition

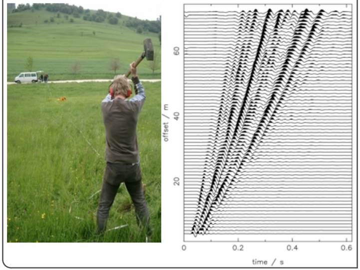

FWI is especially useful to infer <u>small-scale lateral variations</u> and <u>multi-parameter models</u> (V_p, V_s, Q_p, Q_s)

Field laboratory glider field Rheinstetten

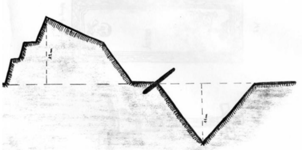

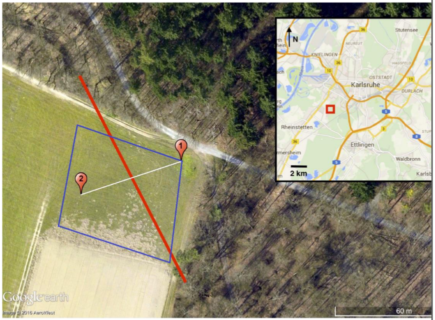

Profile crosses known trench ”Ettlinger Linie” excavated in the 18^{th} century. The trench is 5m wide and 2m deep.

Rayleigh waves

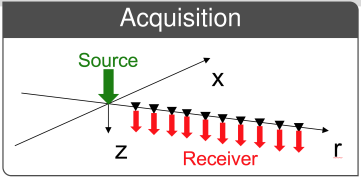

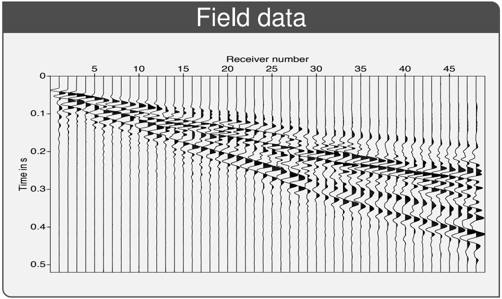

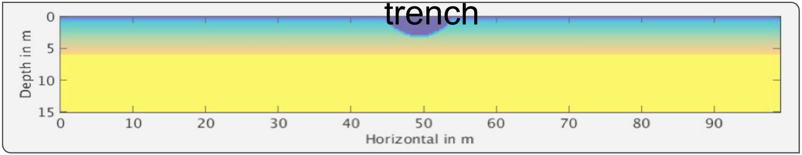

Click to play

Love waves

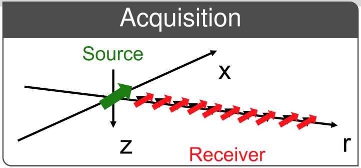

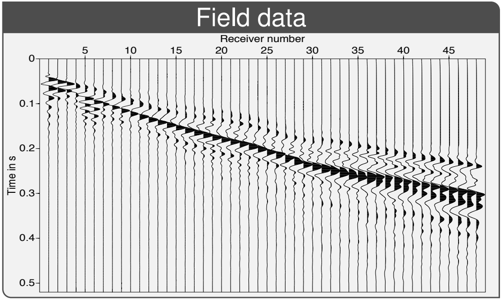

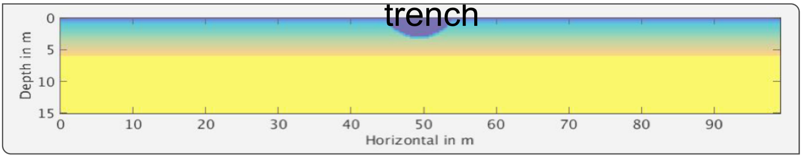

Click to play

Attenuation in the near surface

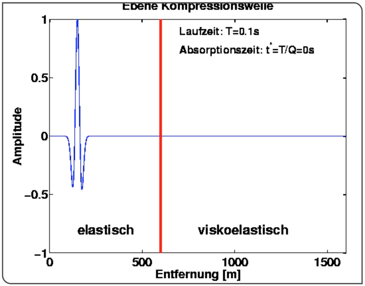

Click to play

Effects of attenuation

1. Amplitude decay with distance
2. Loss of high frequencies with distance
3. Dispersion

must be considered in FWI

Attenuation in the near surface

Effects of attenuation on the observed seismograms

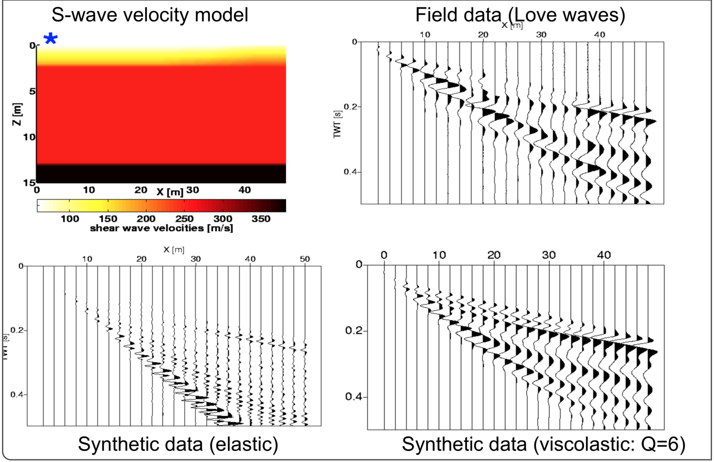

(Bohlen 1998)

First visco-elastic FWI of synthetic data

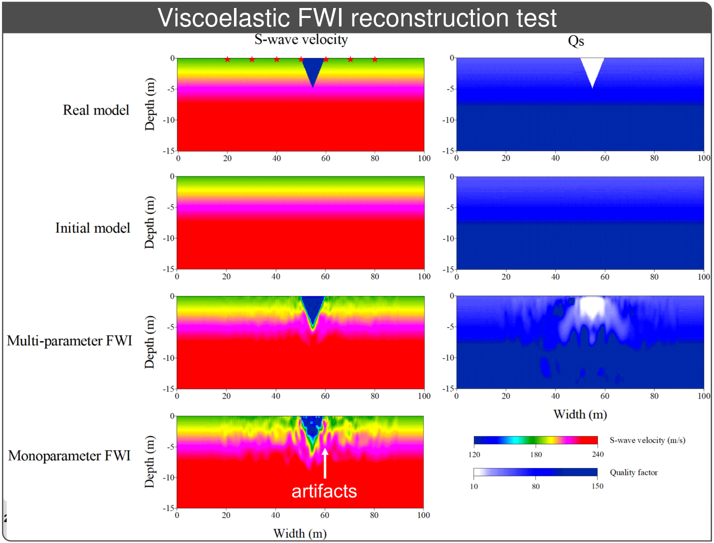

(Gao et al. 2018)

First visco-elastic FWI of field data

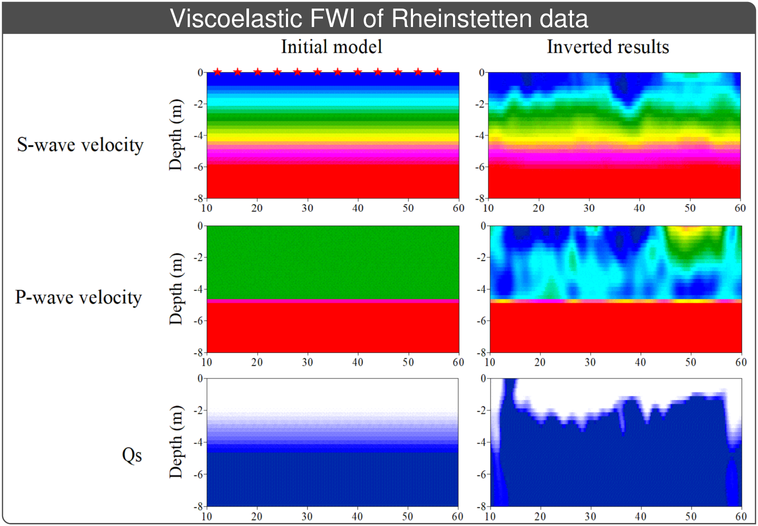

(Gao et al. 2018)

First visco-elastic FWI of field data

Synthetic and field data

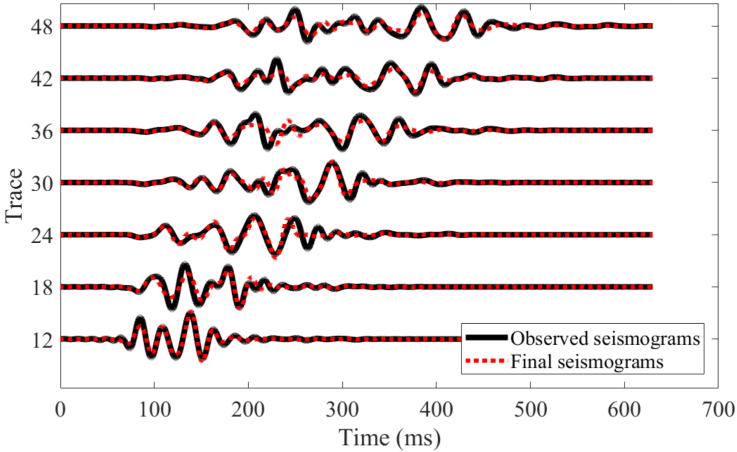

(Gao et al. 2018)

Visco-elastic FWI for near surface characterization

Conclusions

- Visco-elastic FWI can resolve small-scale structures in P-wave and S-wave velocity in the near surface
- Further research is necessary to improve models of attenuation and density

Questions ?

Agenda

Karlsruhe Institute of Technology

Acquisition geometry

Click on frame to play movie

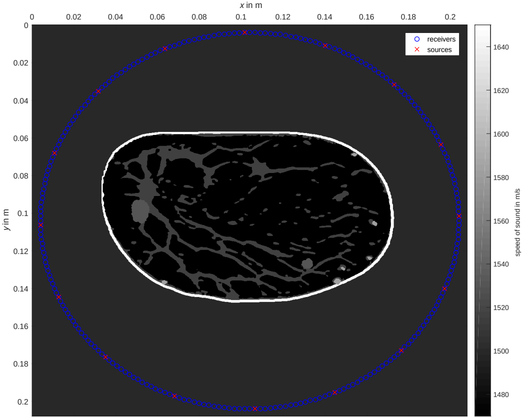

2D acquisition geometry used in the reconstruction test.
The ring array is equipped with 256 receivers and 16 sources.

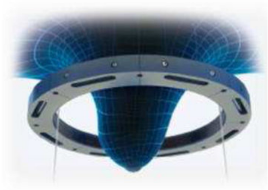

Measurement with a 2D ring transducer
(Sandhu et al., 2015)

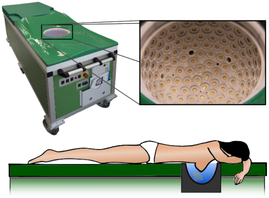

Prototype of a ultrasound device with a full
3D acquisition geometry (Ruiter et al., 2017).
(Kühn 2018)

Reconstruction of speed of sound

Propagation medium	$v_{p,true}$ in m/s	$\overline{v_{p,FWI}}$ in m/s	$\sigma(v_{p,FWI})$ in m/s
Fat	1470	1469	6
Fibroglandluar	1515	1520	13
Tumour	1530	1530	7
Blood vessels	1584	1572	18
Skin	1650	1636	28
Water	1500	NA	NA

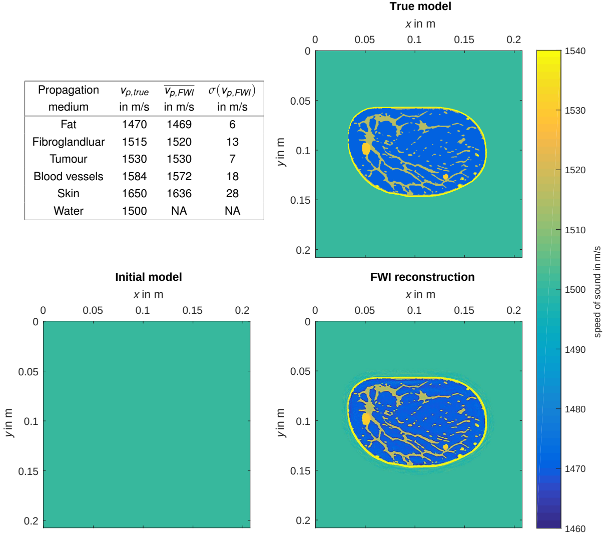

True, initial and inverted speed of sound models (Kühn 2018)

Reconstruction of damping

Propagation medium	$Q_{p,true}$	$\overline{Q_{p,FWI}}$	$\sigma(Q_{p,FWI})$
Fat	462	459	172
Fibroglandluar	279	263	125
Tumour	385	382	109
Blood vessels	>1000	178	83
Skin	644	394	381
Water	>1000	NA	NA

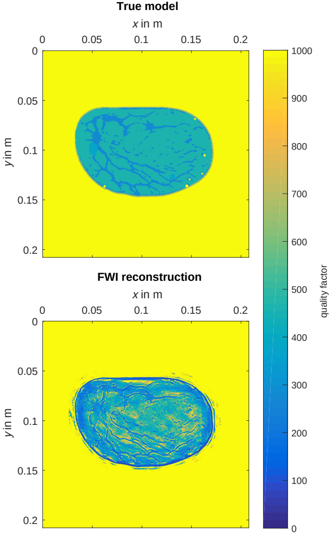

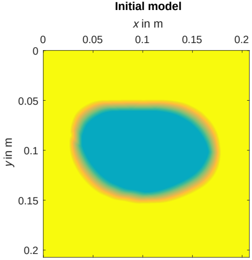

True, initial and inverted quality factor models (Kühn 2018)

Data fit

Data for the true, initial and inverted model

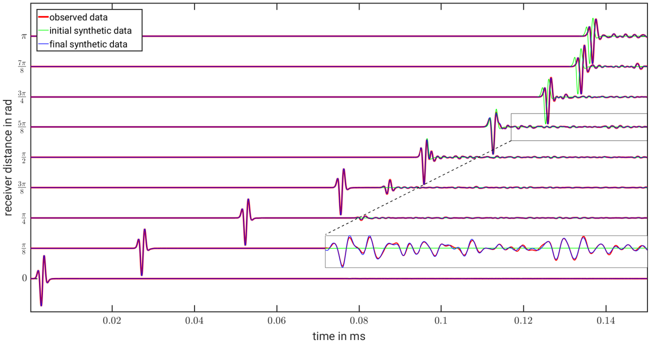

(Kühn 2018)

Visco-acoustic FWI for medical imaging

KIT
Karlsruhe Institute of Technology

Conclusions

- Forward modelling is very expensive due to the high frequencies in medical imaging
- 3D applications are still prohibitive
- 2D visco-acoustic FWI of synthetic data with good illumination works very well
- Detailed models of P-velocity and attenuation can be recovered

Agenda

Karlsruhe Institute of Technology

Conclusions

Karlsruhe Institute of Technology

Summary

First applications revealed that FWI is applicable on different wave types acquired on a broad range of spatial scales. We are still in the early stage of the development of this technology.

Promising directions of future research

- Develop multi-parameter reconstruction techniques
- Integrate constraints from boreholes or other geophysical methods e.g. using cross-gradients
- Joint-inversion with full signals from other geophysical methods (EM, Gravity, ERT)
- Global optimization strategies (independence of initial information, uncertainty estimation)

Acknowledgement

Karlsruhe Institute of Technology

We greatfully acknowledge financial support from

Sponsors of

W I T

Project WAVE

Federal Ministry of Education and Research

CRC 1173

DFG Deutsche Forschungsgemeinschaft

Project SUGAR

Federal Ministry for Economic Affairs and Energy

Thank you for your attention

Thomas.Bohlen@kit.edu
http://www.gpi.kit.edu/

References

Bohlen, T. (1998), Viskoelastische FD-Modellierung seismischer Wellen zur Interpretation gemessener Seismogramme, Dissertation, Christian-Albrechts-Universität zu Kiel.

Forbriger, T., Groos, L. & Schäfer, M. (2014), 'Line-source simulation for shallow-seismic data. Part 1: theoretical background.', *Geophysical Journal International* **198**(3), 1387–1404.

Gao, L., Yudi, P. & Bohlen, T. (2018), 'Reconstructing 2D near-surface models via viscoelastic full waveform inversion of shallow-seismic surface wave', *to be submitted to Geophysical Journal International* .

Gassner, L. (2018), Seismic characterization of submarine gas-hydrate deposits in the Western Black Sea by full-waveform inversion of OBS data, PhD thesis, Karlsruhe Institute of Technology.
URL: *https://publikationen.bibliothek.kit.edu/1000089385*

Gassner, L., Gerach, T., Hertweck, T. & Bohlen, T. (2019), 'Seismic characterization of submarine gas-hydrate deposits in the western black sea by acoustic full-waveform inversion of obs data', *Geophysics (accepted)* .

Habelitz, P. M. (2017), 2D akustische Wellenforminversion geführter Wellen im Flachwasser, Master's thesis, Karlsruhe Institute of Technology.
URL: *https://publikationen.bibliothek.kit.edu/1000080198*

Igel, H., Käser, M. & Stupazzini, M. (2011), *Seismic Wave Propagation in Media with Complex Geometries, Simulation of*, Springer New York, New York, NY, pp. 765–787.
URL: *https://doi.org/10.1007/978-1-4419-7695-6_41*

Kühn, F. (2018), Ultrasound medical imaging using 2d viscoacoustic full waveform inversion, Master's thesis, Karlsruhe Institute of Technology.
URL: *https://publikationen.bibliothek.kit.edu/1000089567*

Kunert, M. (2015), Anwendung der 2D akustischen Wellenforminversion auf OBC-Daten, Master's thesis, Karlsruhe Institute of Technology.
URL: *https://publikationen.bibliothek.kit.edu/1000052718*

Kunert, M., Kurzmann, A. & Bohlen, T. (2016), Application of 2D Acoustic Full Waveform Inversion to OBC-data in Shallow Water, *in* '78th EAGE Conference and Exhibition 2016', EAGE.
URL: *http://earthdoc.eage.org/publication/publicationdetails/?publication=85791*

Schäfer, M., Groos, L., Forbriger, T. & Bohlen, T. (2014), 'Line-source simulation for shallow-seismic data. part 2: full-waveform inversion—a synthetic 2-D case study', *Geophysical Journal International* **198**(3), 1405–1418.
URL: *http://gji.oxfordjournals.org/content/198/3/1405.abstract*

Thiel, N. (2018), Acoustic and elastic FWI of marine dual-sensor streamer data in the presence of salt, PhD thesis, Karlsruher Institut für Technologie (KIT).
URL: *https://publikationen.bibliothek.kit.edu/1000082625*

Thiel, N., Hertweck, T. & Bohlen, T. (2019), 'Comparison of acoustic and elastic full-waveform inversion of 2D towed-streamer data in the presence of salt', *Geophysical Prospecting* **67**, 349–361.
URL: *https://onlinelibrary.wiley.com/doi/abs/10.1111/1365-2478.12728*

Geometrical Spreading Correction

Karlsruhe Institute of Technology

Greens function in 2D and 3D acoustic homogeneous medium

Point source (field data)

$$G^{3D} = \frac{1}{r} e^{ikr}$$

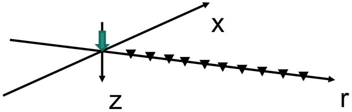

Line source (2D FWI)

$$G^{2D} \simeq \sqrt{\frac{2\pi}{kr}} e^{ikr} e^{i\pi/4}$$

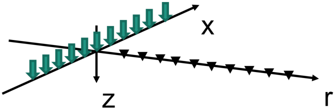

Correction *(Forbriger et al., 2014)*

$$\frac{G^{2D}}{G^{3D}} \simeq \sqrt{\frac{2\pi r}{k}} e^{i\pi/4} \overset{k=\frac{\omega}{c}}{=} \underbrace{\sqrt{2rc}}_{F_{amp}} \underbrace{\sqrt{\frac{\pi}{\omega}} e^{i\pi/4}}_{\tilde{F}\left(\sqrt{t^{-1}}\right)}$$

$$F_{amp} = r\sqrt{2}\sqrt{t^{-1}}$$

far field — near field

(Forbriger et al. 2014)

Geometrical Spreading Correction of Surface Waves

Karlsruhe Institute of Technology

after correction

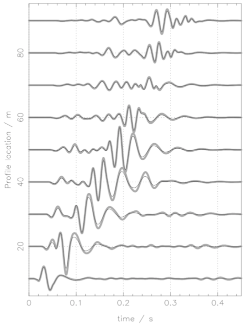

- works surprisingly well for shallow seismic wave fields
- single-trace transformation
- applicable also in case of lateral heterogeneity

line source seismograms

corrected point source seismograms

(Schäfer et al. 2014)